A joint theoretical and experimental study of 1-acetylpiperazine: Conformational stability, infrared and Raman spectra

ARTICLE *in* SPECTROCHIMICA ACTA PART A MOLECULAR AND BIOMOLECULAR SPECTROSCOPY · JUNE 2014

Impact Factor: 2.35 · DOI: 10.1016/j.saa.2014.02.085

5 AUTHORS, INCLUDING:

Metin Bilge
Ege University
11 PUBLICATIONS **6** CITATIONS
SEE PROFILE

Mahir Tursun
Dumlupinar Üniversitesi
18 PUBLICATIONS **35** CITATIONS
SEE PROFILE

Gürkan Keşan
University of South Bohemia in České Bud…
19 PUBLICATIONS **65** CITATIONS
SEE PROFILE

Spectrochimica Acta Part A: Molecular and Biomolecular Spectroscopy 127 (2014) 388–395

Contents lists available at ScienceDirect

Spectrochimica Acta Part A: Molecular and Biomolecular Spectroscopy

journal homepage: www.elsevier.com/locate/saa

A joint theoretical and experimental study of 1-acetylpiperazine: Conformational stability, infrared and Raman spectra

Nesrin Emir [a], Metin Bilge [a], Mahir Tursun [b], Gürkan Keşan [c], Cemal Parlak [b,*]

[a] Department of Physics, Science Faculty, Ege University, İzmir 35100, Turkey
[b] Department of Physics, Dumlupınar University, Kütahya 43100, Turkey
[c] Institute of Physics and Biophysics, Faculty of Science, University of South Bohemia, Branišovská 31, České Budějovice 370 05, Czech Republic

HIGHLIGHTS

- Infrared, Raman and quantum chemical calculations of 1-ap.
- Normal chair form with e–e substituents is not preferred.
- Conformational energy barrier is independent of the solvent.
- Vibrational frequencies and intensities change when going from nonpolar to polar solvents.

GRAPHICAL ABSTRACT

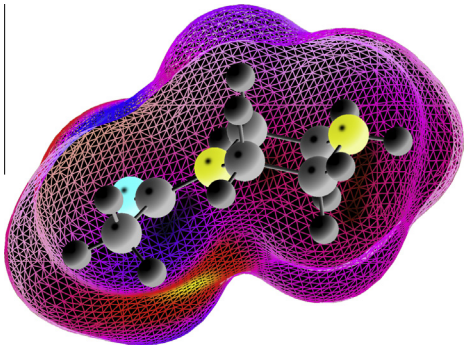

ARTICLE INFO

Article history:
Received 27 November 2013
Received in revised form 28 January 2014
Accepted 19 February 2014
Available online 1 March 2014

Keywords:
1-Acetylpiperazine
Vibrational spectra
DFT
PES
PED

ABSTRACT

Infrared and Raman spectra of 1-acetylpiperazine (1-ap) have been recorded in the region of 4000–40 cm^{-1}. The conformational isomers, optimized geometric parameters, normal mode frequencies and corresponding vibrational assignments of 1-ap ($C_6H_{12}N_2O$) have been examined by density functional theory (DFT), with the Becke-3–Lee–Yang–Parr (B3LYP) functional and the 6-31++G(d,p) basis set. Reliable conformational investigation and vibrational assignments have been performed by the potential energy surface (PES) and potential energy distribution (PED) analyses, respectively. Computations are carried out in both gas phase and solution using benzene and methanol. There is a good agreement between the theoretically predicted structural parameters and vibrational frequencies and those obtained experimentally. The normal chair conformation with equatorial substituents is not preferred due to the steric interaction.

Introduction

1-Acetylpiperazine, called in the literature by different names such as 1-piperazinoethanone, 1-(piperazin-1-yl)ethan-1-one and 1-oxo-1-(piperazin-1-yl)ethane, is a very versatile molecule. It has been the subject of many scientific studies. For example, 1-ap has been used in synthesizing some novel anticancer agent [1], inhibitors of hepatitis C virus [2] and the human pregnane X receptor [3], metal salts [4], mononuclear 3d-transition metal complexes [5], dialkylaminoalkyl derivatives [6], dual cholinesterase and ab-aggregation inhibitors [7]. 1-ap has also been employed in the researching structure–activity relationship on two novel and potent cognition enhancing drugs [8], optimization of surfaces for antibody immobilization using metal complexes [9], HIV-1 integrase inhibitors [10].

* Corresponding author. Tel.: +90 (274) 265 20 31/3116; fax: +90 (274) 265 20 14.
E-mail address: cemal.parlak@dpu.edu.tr (C. Parlak).

http://dx.doi.org/10.1016/j.saa.2014.02.085
1386-1425/

In the literature, there are ample examples of 1-ap being used as an intermediate material in both organic and medicinal chemistry. However, there is lack of information on the vibrational and structural studies of 1-ap in the literature. In the present study, the structure of 1-ap was characterized by vibrational spectroscopy. Further, DFT in conjunction with the B3LYP/6-31++G(d,p) was employed to predict the structural and spectroscopic parameters of the compound in the both gas phase and solution. The findings of these spectroscopic and theoretical studies are herein reported.

Experimental

A commercially available sample of 1-ap in solid form was purchased from Aldrich (99%) and used without further purification. FT-MIR and FT-FIR spectra of 1-ap were recorded in the region of 4000–400 cm^{-1} and 400–40 cm^{-1} with Bruker Optics IFS66v/s FTIR spectrometer at a resolution of 2 cm^{-1}. Raman spectrum was obtained using a Bruker Senterra Dispersive Raman microscope spectrometer with 532 nm excitation from a 3B diode laser having 2 cm^{-1} resolution in the spectral region of 4000–40 cm^{-1}.

Computational details

All the computations were performed using Gaussian 09.A1 program package [11]. GaussView 5.0.8 [12] was used for visualization of the structure and simulation of the vibrational spectra. Several possible isomers could be proposed for 1-ap. However, the discussions are limited only to six isomers, four of them (A: a–e (axial-equatorial), B: a–a, C: e–e, D: e–a, where the former represents NH while the latter stands for acetyl group) from the conformations of piperazine [13] and the other two (E and F) from PES analysis (Fig. 1). A–D forms are considered in axial and equatorial positions according to plane formed by C2, C3, C5 and C6 carbon atoms of 1-ap. We performed the potential energy surface (PES) analysis on the rotations of 6C—5C—4N—13H and 5C—6C—1N—7C torsion angles, scanning from 0° to 180°, with 10° increments. Scan process were conducted for different isomers and it was found that the molecule under investigation is the most stable in the conformer F (Fig. 2, Table 1). Fig. 2 shows PES graphics for 1-ap which allowed us to determine its conformational composition with a high accuracy.

For all the computations, the six isomers of 1-ap were optimized using B3LYP functional in conjunction with the 6-31++G(d,p) basis set both in the gas phase and in benzene and methanol solvent environments. Harmonic vibrational frequencies and their corresponding vibrational intensities were also computed using the same functional and basis set. Vibrational frequencies scaled to generate the corrected frequencies, by 0.955 (>1800 cm^{-1}) and 0.977 (<1800 cm^{-1}) [14–16]. The fundamental normal modes were assigned. PED calculations were carried out by the VEDA 4 (Vibrational Energy Distribution Analysis) as described earlier [17]. Calculated Raman activities are converted to relative Raman intensities using the relationship derived from the intensity theory of Raman scattering [18,19]. The highest occupied and lowest unoccupied molecular orbitals (HOMO and LUMO) of the compound were analyzed.

Results and discussion

The results of the electronic computations on the isomers and geometrical parameters of 1-ap are reported and discussed. This is followed by discussion of the experimental and theoretical vibrational frequencies and their intensities.

Geometrical structures

The energetic and some molecular parameters of the six forms of 1-ap listed in Table 1. Regarding the calculated energies, the F conformer is more stable than others for the all medium. The A–D forms could be neglected for calculation of equilibrium constant since their energy differences are larger than 2 kcal/mol [14,18,20,21]. The F form is more stable than E by 0.704, 0.532

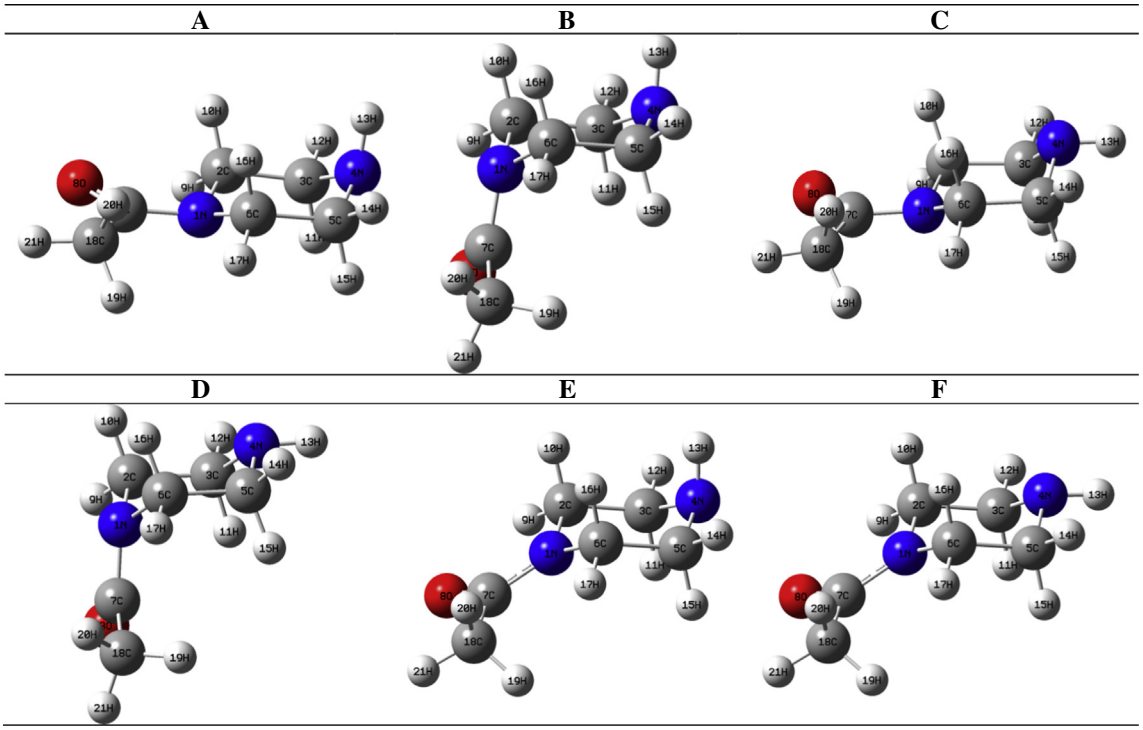

Fig. 1. Optimized structures of the investigated isomers.

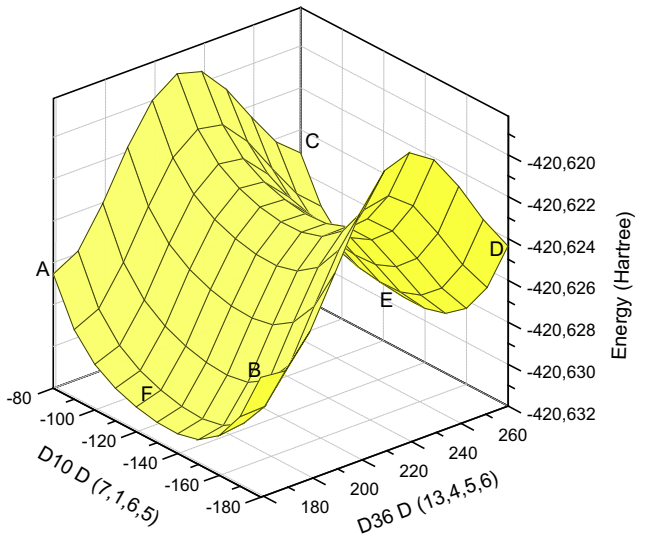

Fig. 2. Potential energy surface for 1-ap.

and 0.248 kcal/mol in various medium. Consequently, 1-ap in the gas phase prefers E and F forms with the approximate preference of 23% and 77% probabilities, respectively. Similarly, in benzene as a non-polar solvent, 1-ap prefers E and F forms with the approximate preference of 29% and 71% probabilities, respectively. The results in methanol as polar solvent also show that the compound prefers E and F forms with the approximate preference of 40% and 60% probabilities, respectively.

The crystal structures of piperazine derivatives showed that the substituents on a piperazine ring generally occupy in the e–e and a–e position [13]. In the case of E and F forms, the NH group is found in the axial (71°) and equatorial (176°) position by 6C—5C—4N—13H, respectively. However, neither axial nor equatorial positions for the acetyl group are favored since the dihedral angles of 5C—6C—1N—7C are calculated as about 136° (Tables 1 and 2). This is due to steric effects of substituents on the piperazine.

To clarify the vibrational frequencies, it is essential to examine the geometry of the compound. A very small change in the geometry can potentially cause substantial variations in their frequencies. Some of the experimental and theoretical (optimized) geometric parameters (bond lengths, bond and torsion angles) are listed in Table 2. To the best of our knowledge, the experimental data on geometric parameters of 1-ap is not available in the literature. Therefore, the theoretical results are compared together with the data of related parts of some molecules such as piperazine, 1-acetyl-3-(2,4-dichloro-5-fluoro-phenyl)-5-phenyl-pyrazoline, 3-N,N-dimethylhydrazino-2-acetyl propenenitrile and (+)-enantiomer of ketoconazole [22–25]. In general, all the calculated parameters are in good agreement with the previously reported experimental data for its fragments [22–25]. The correlation values between the experimental and calculated bond lengths, angles and dihedral angles are found to be 0.97505, 0.97871 and 0.99943, respectively. The lengthening of C=O, shortening of both C—N and C—C bond distances in the condensed phase indicate the strong intermolecular interaction. The bond lengths of CH_3 in crystal are noticeably shorter than liquid or gas partly because the distance of hydrogen atom inherently comes shorter through the crystal packing.

Several thermodynamic parameters (capacity, zero point energy, entropy, etc.) for E and F forms are also presented in Table S1. The variation in the zero point vibrational energy seems to be insignificant. The total energy and change in total entropy of 1-ap are at room temperature. The dipole moment is expected to be larger in solution than the corresponding dipole moment in the gas phase. This situation is clearly observed in Table S1. The dipole moment increases gradually from a lower to a higher dielectric and the increases going from gas to non-polar/polar solvents are about 15%/36% (F) and 17%/42% (E).

Vibrational studies

All the experimental and theoretical vibrational frequencies for 1-ap, along with corresponding vibrational assignments and intensities, are given in Tables 3 and S2. The experimental and simulated vibrational spectra are depicted in Figs. 3–5 and S1. All calculated frequency values presented in this paper are obtained within the harmonic approximation. This allows describing the vibrational motion in terms of independent vibrational modes, each of which is governed by a simple one-dimensional harmonic potential. The compound consists of 21 atoms, having 57 normal vibrational modes, and it belongs to the point group C_1 with only identity (E) symmetry element or operation. It is very difficult to determine the vibrational assignments of 1-ap due to its low symmetry. The assignments of vibrational modes for the investigated isomers

Table 1
Energetic and molecular parameters of 1-ap.

Phase	Conformers	ΔE (Hartree) B3LYP/631++G(d,p)	Relative energy (kcal/mol)	D(C5—C6—N1—C7)	D(C6—C5—N4—H13)
Gas	A	−420.474	3.392	179.9	179.2
	B	−420.474	3.606	79.9	179.2
	C	−420.473	4.190	179.9	179.2
	D	−420.473	4.320	79.9	79.2
	E	−420.479	0.704	136.9	71.2
	F	−420.480	0.000	136.5	175.4
Benzene	A	−420.479	3.380	179.9	179.2
	B	−420.479	3.828	79.9	179.2
	C	−420.478	4.252	179.9	179.2
	D	−420.478	4.360	79.9	79.2
	E	−420.484	0.532	135.3	70.3
	F	−420.485	0.000	135.6	176.2
Methanol	A	−420.486	3.488	179.9	179.2
	B	−420.485	4.230	79.9	179.2
	C	−420.485	4.382	179.9	179.2
	D	−420.485	4.367	79.9	79.2
	E	−420.491	0.248	132.7	69.1
	F	−420.492	0.000	135.0	177.2

Table 2
Some optimized geometric parameters.

Parameters	Experimental [a,b,c,d]		B3LYP/6–31++G(d,p)									
			Gas						Benzene		Methanol	
			A	B	C	D	E	F	E	F	E	F
Bond lenghts (Å)												
N4—H13			1.017	1.016	1.015	1.017	1.018	1.016	1.019	1.016	1.020	1.017
N1—C7	1.340[a]	1.340[d]	1.389	1.387	1.391	1.387	1.376	1.375	1.370	1.369	1.363	1.363
C7=O8	1.217[a]/1.236[b]	1.230[d]	1.228	1.229	1.228	1.229	1.232	1.232	1.237	1.237	1.244	1.244
(C—N)pp	1.467[c]	1.460[d]	1.471	1.472	1.466	1.471	1.465	1.464	1.466	1.466	1.468	1.468
(C—C)pp	1.540[c]	1.505[d]	1.525	1.533	1.534	1.540	1.537	1.530	1.537	1.530	1.537	1.530
(C—H)pp	1.110[c]	0.970[d]	1.098	1.097	1.097	1.096	1.097	1.098	1.096	1.097	1.095	1.097
C7—C18	1.502[a]/1.505[b]	1.511[d]	1.521	1.229	1.228	1.522	1.523	1.523	1.522	1.522	1.520	1.520
C—H_3	0.960[b]	0.960[d]	1.093	1.093	1.094	1.093	1.093	1.093	1.093	1.093	1.093	1.093
Bond angles (°)												
C2—N1—C7		120.5[d]	112.9	115.5	112.7	115.6	119.5	119.5	120.0	119.9	120.6	120.4
C6—N1—C7		126.6[d]	118.5	121.6	118.2	121.7	125.4	125.5	125.3	125.3	125.3	125.1
N1—C7=O8	119.6[a]	121.9[d]	121.6	121.9	121.6	121.8	121.7	121.8	121.7	121.8	121.7	121.7
O8=C7—C18	123.1[a]	120.1[d]	120.9	120.7	120.9	120.8	120.4	120.4	120.3	120.2	120.1	120.1
(C—C—N)pp	110.4[c]	111.1[d]	111.5	109.5	113.8	111.6	112.0	109.8	112.0	109.8	112.0	109.9
(C—N—C)pp	109.0[c]	111.6[d]	112.5	111.3	113.8	111.8	112.9	112.9	112.7	112.7	112.5	112.4
(H—C—H)pp	109.1[c]	108.0[d]	107.7	108.3	107.1	107.7	107.7	108.3	107.8	108.3	107.9	108.2
Dihedral angles (°)												
C2—C3—N4—H13			−177.2	−177.1	−77.1	−76.9	−71.0	−175.4	−70.1	−176.2	−69.1	−177.3
C6—C5—N4—H13			179.2	179.2	79.2	79.2	71.2	175.4	70.3	176.2	69.1	177.2
C3—C2—N1—C7		−130.9[d]	−176.1	−81.9	−176.0	−81.8	−136.0	−136.0	−134.6	−135.1	−132.3	−134.6
C5—C6—N1—C7		132.8[d]	179.9	79.9	179.9	79.9	136.9	136.5	135.3	135.6	132.7	135.0
C2—N1—C7=O8			13.5	−15.0	13.1	−14.8	4.2	4.1	3.6	3.6	2.7	3.1
C6—N1—C7=O8		170.5[d]	153.7	−152.3	152.6	−152.7	173.5	173.8	174.5	174.4	175.8	174.8
C2—N1—C7—C18		−179.3[d]	−168.6	168.9	−169.0	169.0	−176.5	−176.5	−176.9	−176.9	−177.6	−177.3
C6—N1—C7—C18			−28.4	31.5	−29.5	31.1	−7.2	−6.8	−6.1	−6.1	−4.5	−5.6

[a] 1-Acetyl-3-(2,4-dichloro-5-fluoro-phenyl)-5-phenyl-pyrazoline [22].
[b] 3-N,N-dimethylhydrazino-2-acetyl propenenitrile [23].
[c] Piperazine (pp) [24].
[d] (+)-Enantiomer of ketoconazole: (+)-*cis*-1-Acetyl-4-(4-{[(2*R*,4*S*)-2-(2,4-dichlorophenyl)-2-(1*H*-imidazol-1-ylmethyl)-1,3-dioxolan-4-yl] methoxy}phenyl)piperazine[(2*R*,4*S*)-(+)-ketoconazole] [25].

have been provided by VEDA 4. The following are important vibrational motions that were observed.

NH stretching

The free piperazine for the NH equatorial (lone pair axial) conformation has a main NH band at 3351 cm^{-1} with a shoulder at 3314 cm^{-1} in the IR spectrum [26]. For the present molecule, the high frequency region contains characteristic NH stretching bands (ν_1) attributed to piperazine group that are observed at 3318 and 3315 cm^{-1} in the IR and Raman spectra, respectively. The NH stretching is deviated down from the range for piperazine. This is purely due to the impact of acetyl substitution on the ring. The corresponding computed value is calculated at 3385 cm^{-1}. The reason of the difference may be that in the solid state, there are potentially molecular interactions, while in the calculations, the studied molecule is isolated in gas state and there is no other interaction to be considered.

CH stretching

The piperazines exhibit intense perturbed CH bands. This is expected since the substituents are strong electron donors, and all CH_2 groups are adjacent to a N atom. The CH absorption of piperazine is complicated by the existence of conformers with axial or equatorial combinations. The CH_2 stretching bands in the IR spectrum of piperazine were assigned as follows: normal asymmetric mode: 2944 cm^{-1} (perturbed: 2918, 2911 and 2883 cm^{-1}), normal symmetric mode: 2855 cm^{-1} (perturbed: 2825, 2812 and 2749 cm^{-1}) [26]. Similar frequencies are observed for the present compound. CH_2 asymmetric modes (ν_4, ν_6, ν_7) are reported at 2976 (R), 2960/2945 (R/IR), 2952 (R) cm^{-1}. They are calculated at 3009, 2947, 2941 cm^{-1}. CH_2 symmetric modes (ν_9, ν_{11}, ν_{12}) are reported at 2855 (IR), 2817/2814 (IR/R), 2742/2741 (IR/R) cm^{-1}. The computed values at 2882, 2811, 2799 cm^{-1} give excellent agreement with experimental data.

The CH_3 asymmetric and symmetric stretching modes of the acetyl group normally occur in the region of 3020–2960 cm^{-1} and at about 2925 cm^{-1}, respectively [23,27]. CH_3 asymmetric (ν_2) and symmetric (ν_8) bands are observed at 3019/3004 (R/IR) cm^{-1} and 2928/2908 (R/IR) cm^{-1}, respectively. They are consistent with those previously reported data [23,27]. The theoretical values are also found at 3026 and 2911 cm^{-1}, respectively. All the observations indicate that the CH stretching vibrations for the present compounds are within the expected range and there is no considerable impact of substitution on the ring expect for a few obscured asymmetric perturbed CH_2 bands of piperazine by CH_3 symmetric band of acetyl group.

Amide group vibrations

The strong bands in IR/Raman spectra observed at 1635/1615 cm^{-1} are assigned to the amide-I, the C=O stretching band (ν_{13}) of the compound. This assignment is in good agreement with the literature data [22,23,27]. The predicted value is at 1681 cm^{-1} for the gas state. However, there are potentially molecular interactions occurring on O atoms, which finally influence the C=O stretch vibration frequency, in the solid state. The compound shows that the amide-I, band is to be pure even though it has slightly mixed with the CN stretching mode. The amide CN stretching bands (ν_{21}, ν_{29}) are assigned to the wavenumber observed at 1427 (IR), 1247/1245 (IR/R) cm^{-1}. The computed values at 1427 and 1238 cm^{-1} also give excellent agreement with experimental data. The C=O in-plane bending (ν_{45}) and out of plane bending (ν_{46}) modes are calculated to be at 594 and 575 cm^{-1} and

Table 3
Vibrational frequencies (cm^{-1}) for F and E isomers.

Modes	Experimental (Solid)		B3LYP/6-31++G(d,p)–gas phase							
	IR	Raman	F isomer				E isomer			
			Assignments PED[a] (⩾10)	ν[b]	I_{IR}[c]	I_R[c]	Assignments PED[a] (⩾10)	ν[b]	I_{IR}[c]	I_R[c]
ν_1	3318	3315	ν NH (100)	3385	0.58	22.81	ν NH (100)	3349	0.46	15.28
ν_2	3004	3019	ν CH_3 (90)	3026	6.73	13.22	ν CH_3 (91)	3026	6.69	13.61
ν_3	–	–	ν CH_2 (96)	3012	5.84	8.11	ν CH_2 (96)	3001	7.51	9.48
ν_4	–	2976	ν CH_2 (97)	3009	15.13	12.43	ν CH_2 (96)	2997	17.67	17.14
ν_5	–	–	ν CH_3 (95)	2971	12.02	9.25	ν CH_3 (92)	2971	12.10	9.31
ν_6	2945	2960	ν CH_2 (100)	2947	37.75	29.51	ν CH_2 (100)	2955	37.41	23.50
ν_7	–	2952	ν CH_2 (97)	2941	40.50	28.84	ν CH_2 (91)	2950	39.63	23.68
ν_8	2908	2928	ν CH_3 (91)	2911	8.47	28.56	ν CH_2 (91)	2911	7.50	27.43
ν_9	2855	–	ν CH_2 (93)	2882	59.45	26.50	ν CH_2 (87)	2903	40.58	31.35
ν_{10}	–	–	ν CH_2 (94)	2872	40.31	18.83	ν CH_2 (86)	2896	37.16	15.60
ν_{11}	2817	2814	ν CH_2 (94)	2811	87.93	39.13	ν CH_2 (91)	2848	74.53	43.36
ν_{12}	2742	2741	ν CH_2 (95)	2799	69.14	23.18	ν CH_2 (91)	2838	44.09	20.55
ν_{13}	1635	1615	ν CO(92)	1681	397.17	7.32	ν CO (83)	1681	395.09	7.47
ν_{14}	–	1471	β CH_2 (60) + β CH_3 (33)	1475	2.01	5.04	β CH_2 (44) + β CH_3 (44)	1471	2.49	3.29
ν_{15}	1468	–	β CH_2 (55) + β CH_3 (32)	1470	2.27	2.92	β CH_2 (39) + β CH_3 (35)	1465	5.95	2.69
ν_{16}	–	–	γ CH_3 (87)	1463	14.53	0.65	γ CH_3 (87)	1456	15.25	3.94
ν_{17}	–	–	γ CH_3 (71) + γ CH_2 (12)	1459	7.58	6.20	γ CH_3 (85) + γ CH_2 (10)	1454	10.47	1.87
ν_{18}	–	–	γ CH_3 (86)	1453	3.85	7.17	ΔHCH (88)	1448	1.50	2.53
ν_{19}	–	1457	γ CH_3 (96)	1447	3.82	5.31	γ CH_3 (97)	1444	12.61	2.98
ν_{20}	–	1446	β NH (94)	1444	17.75	3.10	β NH (92)	1442	5.50	13.02
ν_{21}	1427	–	ν CN (82) + γ CH_2 (12)	1427	221.71	3.55	ν CN (60) + γ CH_2 (20)	1423	226.10	4.73
ν_{22}	–	1390	γ CH_2 (88) + ν CN (10)	1393	0.36	1.80	γ CH_2 (81) + ν CN (10)	1368	8.80	2.97
ν_{23}	–	–	β CH_3 (68) + γ CH_2 (13)	1368	7.71	0.74	β CH_3 (65) + γ CH_2 (25)	1364	1.63	3.59
ν_{24}	1364	1362	β CH_3 (84)	1360	6.92	0.69	β CH_3 (73)	1359	5.96	0.53
ν_{25}	1339	–	γ CH_2 (89)	1338	21.19	0.51	γ CH_2 (91)	1343	8.33	0.64
ν_{26}	1320	1322	γ CH_2 (90)	1320	27.19	1.27	γ CH_2 (90)	1322	0.88	1.77
ν_{27}	1286	1284	γ CH_2 (75)	1283	23.92	10.22	γ CH_2 (77)	1314	1.89	6.15
ν_{28}	1265	1254	ν CN (64) + β CH_2 (16) + β CO (10)	1262	49.65	1.13	ν CN (64) + β CH_2 (24)	1266	45.39	1.20
ν_{29}	1247	1245	ν CN (54) + γ CH_2 (41)	1238	121.22	7.01	ν CN (48) + γ CH_2 (33)	1237	184.65	9.74
ν_{30}	1200	1200	γ CH_2 (88)	1197	1.64	8.30	γ CH_2 (90)	1190	1.61	1.49
ν_{31}	1166	1178/1165	ν CN (74) + γ CH_2 (23)	1161	13.25	1.72	ν CN (70) + γ CH_2 (21)	1181	7.70	5.35
ν_{32}	1143	1144	ν CN (84)	1137	25.42	1.41	ν CN (80)	1132	1.31	3.44
ν_{33}	1123	1119	β CH_2 (82) + ν CN (10)	1110	10.99	2.47	β CH_2 (65) + ν CN(18)	1118	34.52	0.41
ν_{34}	1058	1058	ν CC (58) + β CN (22) + β CH_2 (10)	1062	4.97	1.97	ν CC (58) + β CN (28) + β CH_2 (10)	1050	2.98	4.94
ν_{35}	–	–	β CH_2 (65) + ν CN (20)	1051	0.48	0.20	β CH_2 (51) + ν CN (20)	1025	2.54	0.16
ν_{36}	1034	–	ν CC (90)	1038	19.28	7.48	ν CC (95)	1008	6.45	1.25
ν_{37}	1015	1017	β CH_3 (84)	1025	3.06	0.25	β CH_3 (80) + ν CN (10)	1000	15.63	5.83
ν_{38}	996	999	β CH_3 (80) + ν CC (11)	984	55.82	1.27	β CH_3 (85) + ν CC (11)	980	41.35	3.81
ν_{39}	966	958	ν CC (91)	948	1.22	4.12	ν CC (80)	945	1.17	4.23
ν_{40}	890	909	ν CC (75) + β CN (15)	895	0.38	2.96	ν CC (74)	887	2.52	2.87
ν_{41}	–	885	ν CC (86)	858	1.89	7.42	ν CC (77) + β CN (14)	853	6.66	7.84
ν_{42}	–	848	ν CC (73) + β CC (23)	838	0.16	0.40	ν CC (70) + β CC (12) + ν CN (10)	819	0.23	0.87
ν_{43}	814	811	ν CC (64) + β CN (27)	763	87.39	4.42	ν CC (65) + β CN (17)	756	155.37	3.32
ν_{44}	716	721	τ CNCC(87) + β CO (10)	706	1.56	17.82	τ CNCC (90)	696	10.68	19.52
ν_{45}	614	615	β CO (68) + β CN (19)	594	1.29	7.23	β CO (70) + β CN (25)	596	14.49	5.13
ν_{46}	591	598	γ CO (62) + τ HCCN (17) + τ HCNC (11)	575	6.00	1.75	γ CO (60) + τ HCCN (20) + τHCNC (11)	574	12.24	1.47
ν_{47}	561	568	γ NH (80) + τ NCCN (13)	534	44.32	4.61	γ NH (78) + τ NCCN (10)	549	1.18	2.23
ν_{48}	484	488	β CC (34) + τ CNCN (30)	469	10.69	2.60	τ CCNC (57) + β CC (12)	471	0.77	2.51
ν_{49}	460	455	β CC (39) + τ CNCN (32)	447	1.85	7.36	τ HCNC (51) + β CC (24)	451	6.73	8.41
ν_{50}	394	440	γ CC (37) + τ CNCN (30)	404	0.40	2.43	γ CC (34) + τ CNCN (30)	389	10.16	1.72
ν_{51}	357	385	τ CNCN (60) + ν CN (22) + β CO (10)	354	1.83	11.05	τ CNCN (66) + ν CN (21) + β CO (10)	354	2.16	13.93
ν_{52}	315	302	β CC (84)	294	4.16	1.22	β CC (78)	291	3.31	0.82
ν_{53}	249	–	β CN (84)	266	7.50	0.83	β CN (84)	263	7.46	3.37
ν_{54}	–	220	γ CC (64) + τ NCCN (27)	207	3.62	0.97	γ CC (60) + τ NCCN (22)	197	2.41	1.71
ν_{55}	191	–	τ CH_3 (92)	175	0.47	3.48	τ CH_3 (88)	172	0.44	2.61
ν_{56}	107	107	τ OCNC (72) + β CO (22)	97	3.51	8.97	τ OCNC (70) + β CO (23)	96	3.46	8.50
ν_{57}	72	63	τ CCNC (94)	53	0.89	77.64	τ CCNC (91)	52	2.25	74.14

[a] PED data are taken from VEDA4.
[b] Scaled frequencies with 0.955 above 1800 cm^{-1}, 0.977 under 1800 cm^{-1}.
[c] I_{IR} and I_R: Calculated infrared (km/mol) and Raman (Å/amu) intensities. ν, β, γ, and τ denote stretching, in plane bending, out of plane bending and torsion, respectively.

correspond to 615/614 (R/IR) cm^{-1} and 598/591 (R/IR) cm^{-1} in the experimental spectra, respectively.

Other vibrations

CH_2 bending bands are assigned as follows; scissoring mode (ν_{14}, ν_{15}): 1471 (R), 1468 (IR) cm^{-1} (1475, 1470 cm^{-1}), wagging mode (ν_{22}, ν_{25}, ν_{26}): 1390 (R), 1339 (IR), 1322/1320 (R/IR) cm^{-1} (1393, 1338, 1320 cm^{-1}), twisting mode (ν_{27}, ν_{30}): 1286/1284 (IR/R), 1200 (IR/R) cm^{-1} (1283, 1197 cm^{-1}) and rocking mode (ν_{33}): 1123/1119 (IR/R) cm^{-1} (1110 cm^{-1}). The computed values in parenthesis are in good agreement with the experimental data. The Raman band at 1446 cm^{-1} is assigned to in-plane bending (ν_{20}) modes of NH whereas the IR/Raman bands at 561/568 cm^{-1} are assigned to NH out-of-plane bending (ν_{47}) band. The theoretical values are 1444 and 534 cm^{-1}. CH_3 asymmetric (ν_{19}), symmetric (ν_{24}) and rock bending (ν_{37}, ν_{38}) are assigned to 1457 (R), 1364/

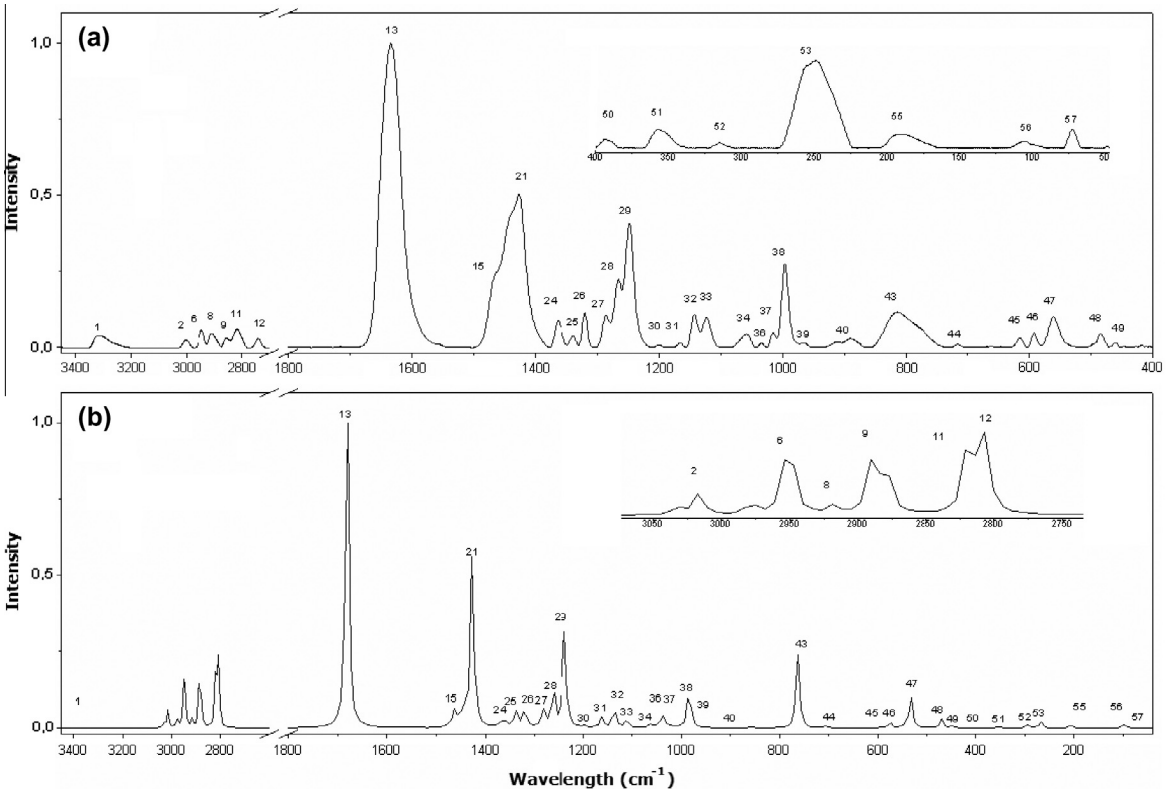

Fig. 3. (a) Experimental and (b) theoretical IR spectra for 1-ap.

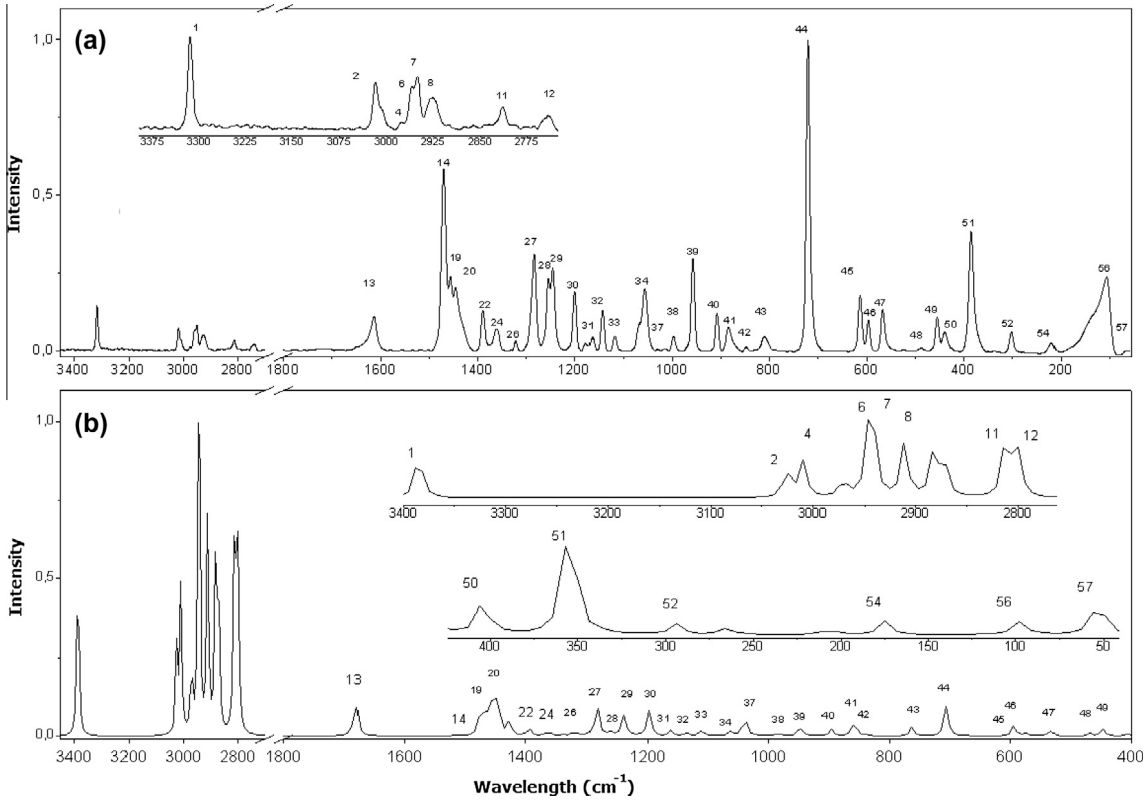

Fig. 4. (a) Experimental and (b) theoretical Raman spectra for 1-ap.

1362 (IR/R) and 1017/1015 (R/IR), 999/996 (R/IR) cm^{-1}, respectively. They are computed at 1447, 1360, 1025, 984 cm^{-1}. The assignment of the band at 191 (ν_{55}) cm^{-1} of IR is attributed to the torsion CH_3. This band is computed at 175 cm^{-1}.

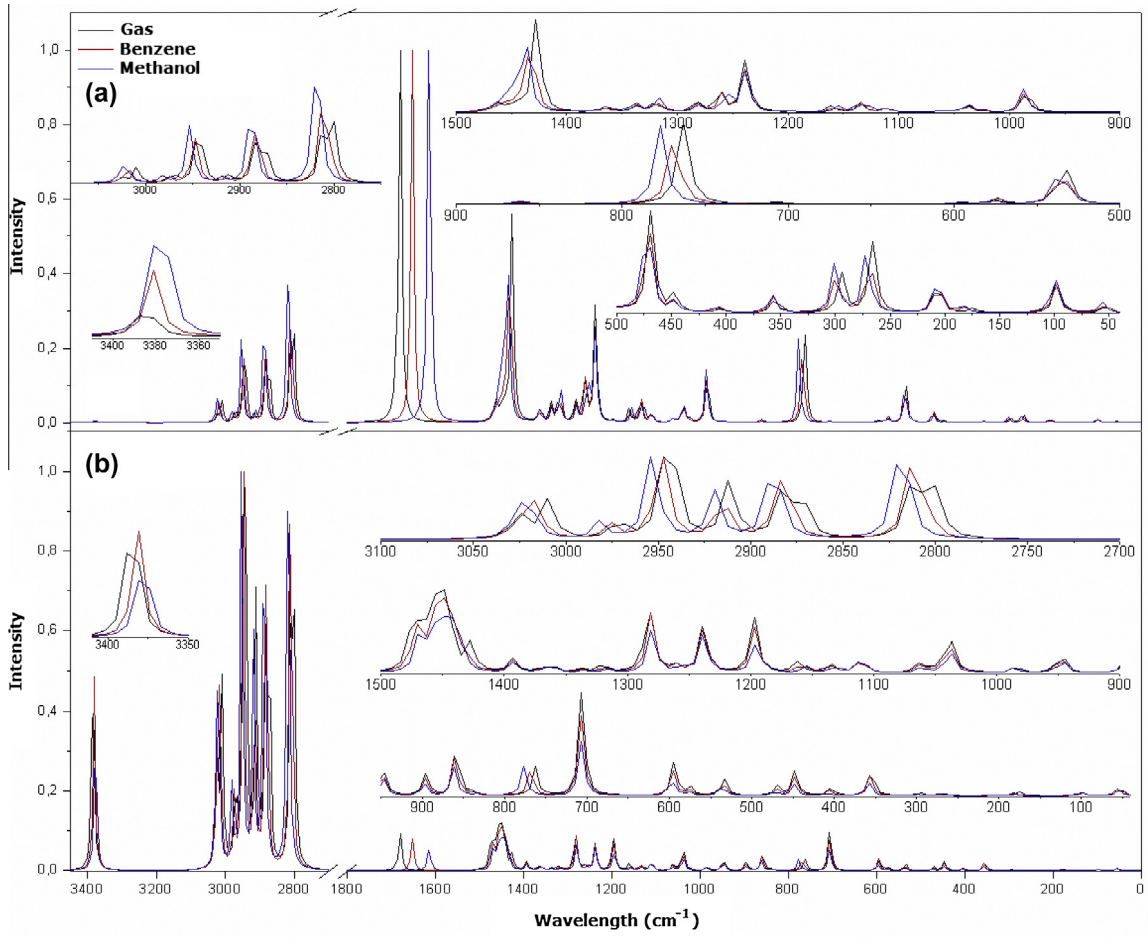

Fig. 5. Theoretical (a) IR and (b) Raman spectra for F form in various medium.

The identification of CN vibrations is a very difficult task since the mixing of several bands is possible in this region. However, with the help of theoretical calculations, the CN stretching vibrations (ν_{28}, ν_{31}, ν_{32}) are assigned at 1265/1254 (IR/R), 1178/1165/1166 (R/R/IR), 1144/1143 (R/IR) cm^{-1}. Similar data have been shown in calculations. The CC stretching modes dominate the regions of 1060–800 cm^{-1} while the CCO, CNC, CCN, HCN or HCH bending and HCCN, CNCN, CCNC or OCNC torsion modes are seen in the low frequency region. Similar situations have been shown in calculations. Hence, for this section, the vibrational frequencies observed in this study are also in agreement with the literature data [13,22,23,27,28].

Solvent effect

The assignments in various medium are generally consistent with one another if the vibrational assignments are investigated one-by-one (Table 3 and Fig. 5). As the presence of dielectric medium has a strong influence on the vibrational frequencies, there are significant changes in the presented theoretical vibrational values. Some important vibrational motions are here described. The C═O and NH bond lengths increase on going from the gas phase to the solvent phase. Therefore, the C═O and NH stretching frequencies should decrease. It is clearly observed that these requirements are substantially fulfilled for 1-ap. These frequencies shifts are explained in terms of increased positive character on oxygen or nitrogen atoms in solvents of high dielectric constant [14].

The computed vibrational intensities in the gas phase are in reasonable agreement with the experimental results in both high and low frequency regions. IR intensities are expected to dramatically change when the solute is solvated and this is indeed the case in our present study. It is seen from Tables 3 and S2 and Figs. 5 and S1 that there are noticeable changes in many modes and the calculated intensities in solutions are very high when compared to those in the gas phase for most cases. Like IR intensities, significant changes in Raman intensities are seen when the molecule is solvated. For the IR/Raman intensities, the increases in methanol are generally larger than in benzene. On the other hand, frontier molecular orbital energy and energy gap of all conformations in various medium is also given as supplementary material (Table S3 and Fig. S2).

Conclusion

The experimental and theoretical vibrational investigations of 1-ap are successfully performed by FT-IR, Raman and quantum chemical computations. Any differences observed between the experimental and computed values may be due to the fact that the computations were performed for a single molecule in the gas and solvations states, whereas the experimental values in the solid phase were recorded in the presence of intermolecular interactions. To summarize, the following conclusions can be drawn:

1. The normal chair conformation with e–e substituents is not preferred. The F form is the most stable isomer of 1-ap. The conformational energy barrier is independent of the solvent. However, the compound tends to be more stable, as the polarity of the solvents increases.

2. It is worth to note that the F conformer has a large dipole moment (4.15 Debye) and this is an essential criteria for drug-receptor interaction [29].
3. Some significant changes are found in the geometric parameters when 1-ap in solvated. From lower to higher dielectric, the dipole moment increases. In general, the frequency differences increase when going from non-polar to polar solvents. Also, solvent effects on vibrational intensities are also considerable and they increase as one goes from lower to higher dielectric constant in the most cases.
4. The following mean absolute deviations (MAD) between the experimental and calculated frequencies (IR/R) are found: 14.50/19.90, 13.80/15.70, 14.60/14.40 cm^{-1} for F form in the gas phase, benzene and methanol. Also, the correlation values (R^2) for IR/R are found: 0.99964/0.99952, 0.99970/0.99963, 0.99966/0.99969, respectively.
5. The B3LYP/6-31++G(d,p) computations are reliable and complement in understanding the vibrational spectra and structural parameters of the investigated compound.

Appendix A. Supplementary material

Supplementary material associated with this article can be found, in the online version, at http://dx.doi.org/10.1016/j.saa.2014.02.085.

References

[1] Y. Wang, J. Ai, Y. Wang, Y. Chen, L. Wang, G. Liu, M. Geng, A. Zhang, J. Med. Chem. 54 (2011) 2127–2142.
[2] M.G. LaPorte, T.A. Lessen, L. Leister, D. Cebzanov, E. Amparo, C. Faust, D. Ortlip, T.R. Bailey, T.J. Nitz, S.K. Chunduru, D.C. Young, C.J. Burns, Bioorg. Med. Chem. Lett. 16 (2006) 100–103.
[3] B.C. Das, A.V. Madhukumar, J. Anguiano, S. Kim, M. Sinz, T.A. Zvyaga, E.C. Power, C.R. Ganellin, S. Mani, Bioorg. Med. Chem. Lett. 18 (2008) 3974–3977.
[4] Q. Wang, C. Wilson, A.J. Blake, S.R. Collinson, P.A. Taskerb, M. Schröder, Tetrahedron Lett. 47 (2006) 8983–8987.
[5] A. Mohammad, C. Varshney, S.A.A. Nami, Spectrochim. Acta A 73 (2009) 20–24.
[6] J. Faist, W. Seebacher, M. Kaiser, R. Brun, R. Saf, R. Weis, Bioorg. Med. Chem. 18 (2010) 6796–6804.
[7] T. Mohamed, J.C.K. Yeung, P.P.N. Rao, Bioorg. Med. Chem. Lett. 21 (2011) 5881–5887.
[8] S. Scapecchi, E. Martini, D. Manetti, C. Ghelardini, C. Martelli, S. Dei, N. Galeotti, L. Guandalini, M.N. Romanelli, E. Teodoria, Bioorg. Med. Chem. 12 (2004) 71–85.
[9] B.W. Muir, M.C. Barden, S.P. Collett, A.D. Gorse, R. Monteiro, L. Yang, N.A. McDougall, S. Gould, N.J. Maeji, Anal. Biochem. 363 (2007) 97–107.
[10] J.P. Guare, J.S. Wai, R.P. Gomez, N.J. Anthony, S.M. Jolly, A.R. Cortes, J.P. Vacca, P.J. Felock, K.A. Stillmock, W.A. Schleif, G. Moyer, L.J. Gabryelski, L. Jin, I. Chen, D.J. Hazuda, S.D. Young, Bioorg. Med. Chem. Lett. 16 (2006) 2900–2904.
[11] M.J. Frisch, G.W. Trucks, H.B. Schlegel, G.E. Scuseria, M.A. Robb, J.R. Cheeseman, G. Scalmani, V. Barone, B. Mennucci, G.A. Petersson, H. Nakatsuji, M. Caricato, X. Li, H.P. Hratchian, A.F. Izmaylov, J. Bloino, G. Zheng, J.L. Sonnenberg, M. Hada, M. Ehara, K. Toyota, R. Fukuda, J. Hasegawa, M. Ishida, T. Nakajima, Y. Honda, O. Kitao, H. Nakai, T. Vreven, J.A. Montgomery Jr., J.E. Peralta, F. Ogliaro, M. Bearpark, J.J. Heyd, E. Brothers, K.N. Kudin, V.N. Staroverov, R. Kobayashi, J. Normand, K. Raghavachari, A. Rendell, J.C. Burant, S.S. Iyengar, J. Tomasi, M. Cossi, N. Rega, J.M. Millam, M. Klene, J.E. Knox, J.B. Cross, V. Bakken, C. Adamo, J. Jaramillo, R. Gomperts, R.E. Stratmann, O. Yazyev, A.J. Austin, R. Cammi, C. Pomelli, J.W. Ochterski, R.L. Martin, K. Morokuma, V.G. Zakrzewski, G.A. Voth, P. Salvador, J.J. Dannenberg, S. Dapprich, A.D. Daniels, Ö. Farkas, J.B. Foresman, J.V. Ortiz, J. Cioslowski, D.J. Fox, Gaussian 09, Revision A.1, Gaussian Inc., Wallingford CT, 2009.
[12] R.D. Dennington, T.A. Keith, J.M. Millam, GaussView 5.0.8, Gaussian Inc., 2008.
[13] Ö. Alver, C. Parlak, M. Şenyel, Spectrochim. Acta A 67 (2007) 793–801.
[14] E. Güneş, C. Parlak, Spectrochim. Acta A 82 (2011) 504–512.
[15] M.F. Kaya, C. Parlak, G. Keşan, Ö. Alver, M. Tursun, Spectrochim. Acta A 113 (2013) 1–9.
[16] M. Tursun, G. Keşan, C. Parlak, M. Şenyel, Spectrochim. Acta A 114 (2013) 668–680.
[17] M.H. Jamróz, Spectrochim. Acta A 114 (2013) 220–230.
[18] Ö. Alver, C. Parlak, Vib. Spectrosc. 54 (2010) 1–9.
[19] G. Keresztury, S. Holly, J. Varga, G. Besenyei, A.Y. Wang, J.R. Durig, Spectrochim. Acta A 49 (1993) 2007–2026.
[20] C. Parlak, J. Mol. Struct. 966 (2010) 1–7.
[21] Ö. Alver, C. Parlak, J. Theor. Comput. Chem. 9 (2010) 667–685.
[22] F. Jian, P. Zhaoa, H. Guob, Y. Li, Spectrochim. Acta A 69 (2008) 647–653.
[23] M. Gróf, A. Gatial, V. Milata, N. Prónayová, J. Kozíšek, M. Breza, P. Matejka, J. Mol. Struct. 938 (2009) 97–110.
[24] A. Yokazeki, K. Kuchitsu, Bull. Chem. Soc. Jpn. 44 (1971) 2352–2355.
[25] O.M. Peeters, N.M. Blaton, J.G. Gerberb, J. Gal, Acta Cryst. E60 (2004) 367–369.
[26] P.J. Krueger, J. Jan, Can. J. Chem. 48 (1970) 3236–3248.
[27] A. Sharma, V. Gupta, P. Tandon, P. Rawat, S. Maeda, K.K. Kunimoto, Spectrochim. Acta A 90 (2012) 141–151.
[28] V. Krishnakumar, S. Seshadri, Spectrochim. Acta A 68 (2007) 833–838.
[29] E.J. Lien, Z.R. Guo, R.L. Li, C.T. Su, J. Pharm. Sci. 71 (1982) 641–655.